JACS
JOURNAL OF THE AMERICAN CHEMICAL SOCIETY

Article

Cross-linked artificial enzyme crystals as heterogeneous catalysts for oxidation reactions

Sarah Lopez, Laurianne Rondot, Chloé Leprêtre, Caroline Marchi-Delapierre, Stéphane Ménage, and Christine Cavazza

J. Am. Chem. Soc., **Just Accepted Manuscript** • DOI: 10.1021/jacs.7b09343 • Publication Date (Web): 17 Nov 2017

ACS Publications

Journal of the American Chemical Society is published by the American Chemical Society. 1155 Sixteenth Street N.W., Washington, DC 20036

Cross-linked artificial enzyme crystals as heterogeneous catalysts for oxidation reactions

by Sarah Lopez,[1,2,3] Laurianne Rondot, [1,2,3] Chloé Leprêtre, [1,2,3] Caroline Marchi-Delapierre, [1,2,3] Stéphane Ménage*,[1,2,3] Christine Cavazza [1,2,3] *

[1] Univ. Grenoble Alpes, F-38000 Grenoble, France.
[2] CEA, BIG, Laboratory of Chemistry and Biology of Metals, BioCE and BioCat group F-8054 Grenoble, France.
[3] CNRS, UMR5249, F-38054 Grenoble, France

Abstract: Designing systems that merge the advantages of heterogeneous catalysis, enzymology and molecular catalysis represents the next major goal for sustainable chemistry. Cross-linked enzyme crystals display most of these essential assets (well-designed mesoporous support, protein selectivity, molecular recognition of substrates). Nevertheless, a lack of reaction diversity, particularly in the field of oxidation, remains a constraint for their increased use in the field. Here, thanks to the design of cross-linked artificial non-heme iron oxygenase crystals, we filled this gap by developing bio-based heterogeneous catalysts capable of oxidizing carbon-carbon double bonds. First, reductive O_2 activation induces selective oxidative cleavage, revealing the indestructible character of the solid catalyst (at least 30 000 turnover numbers without any loss of activity). Second, the use of 2-electron oxidants allows selective and high-efficiency hydroxychlorination with thousands of turnover numbers. This new technology by far outperforms catalysis using the inorganic complexes alone, or even the artificial enzymes in solution. The combination of easy catalyst synthesis, the improvement of "omic" technologies and automation of protein crystallization makes this strategy a real opportunity for the future of (bio)catalysis.

Introduction

Catalysis represents a cornerstone of chemical synthesis in a sustainable world.[1] Tremendous achievements have been made by using biocatalysts, which combine mild conditions, high catalytic cycle number and selectivity, in particular for reduction or oxidation processes.[2] To ensure their relevance for industry, enzyme immobilization is often a pre-requisite, maximizing reusability, avoiding enzyme precipitation and improving the biocatalyst's performance.[3] Basically, three traditional methods of enzyme immobilization can be distinguished: covalent (in)organic material, entrapment (e.g. silica gel) and cross-linking. Cross-linking consists of attaching proteins to each other by a covalent bond, using a bifunctional reagent, frequently glutaraldehyde which reacts preferentially with the ε-amino groups of lysine residues.[3b,4] Among the different strategies tested to date, cross-linked enzyme aggregates (CLEAs) are used as a simpler alternative with a certain level of success, mostly for hydrolytic reactions (lipase, invertase, hydroxynitrile lyase, cellulase) or reduction reactions (alcohol dehydrogenase). In contrast, oxidation reactions - major transformations in organic synthesis - are rather scarce, with the exception of a few heme enzymes.[3a,5] An alternative to CLEAs is the Cross-Linked Enzyme Crystals (CLEC) approach, which combines the advantages of enzymology and heterogeneous catalysis.[6] In CLEC, the high chemo-, regio- and enantio-selectivity of the enzyme is combined with a high protein concentration in mesoporous microcrystals. The high solvent content of protein crystals allows mass transfer from the surface to the active sites, preserves the high catalytic efficiency of the enzyme and affords remarkable stability, allowing the use of a large range of solvents and thus substrates, without requiring expensive supports. CLEC technology has been applied in chiral resolution, peptide synthesis (subtilisin, thermolysin)[7] and biosensing applications (Glucose oxidase)[8], but only one example of an oxygen transfer reaction has been described to date.[9] This reaction relied on chloroperoxidase, and its activity was low. This biotechnological method may be renewed through the development of artificial metalloenzymes, a hybrid biomaterial formed by embedding an inorganic catalyst (playing the role of the active site) within a protein scaffold (to drive reaction selectivity). This approach could produce new biomimetic reactions to achieve non-natural catalysis or to propose higher catalytic performance in terms of efficiency, stability and recycling.[10] Up to now, only one example of CLEC using an artificial metalloenzyme has been described. This system catalyzes the moderate enantioselective reduction of ketones and was produced by soaking hen egg white lysozyme crystals with Ru(benzene)Cl_2 complexes.[11]

Here, we report the design of unique heterogeneous catalysts, based on the use of

cross-linked NikA crystals. NikA is a 56 kDa periplasmic nickel-binding protein involved in nickel import in *Escherichia coli*. Like other extra-cytoplasmic binding proteins, NikA is composed of two lobes connected by a hinge, in which the ligand is located (Figure S1 and S2). Based on our previous studies showing that the protein is able to bind non-physiological Fe-EDTA-like catalysts[12], we synthesized a series of **NikA/Fe-Lx (x= 0-2) CLEC**. Our results reveal the outstanding performance of **NikA/Fe-L2 CLEC** for oxidative alkene cleavage by dioxygen, highlighting the high recycling properties of the catalytic biomaterial. In addition, we demonstrated the versatility of **NikA/Fe-L2 CLEC** for a panel of oxidative transformations of carbon-carbon double bonds - a major transformation in organic synthesis[13] - including oxidative cleavage, enol ether oxidation and hydroxychlorination under mild conditions.

Figure 1. Activation of molecular O_2 by NikA/Fe-L0 crystals and presentation of the complexes used in this study.

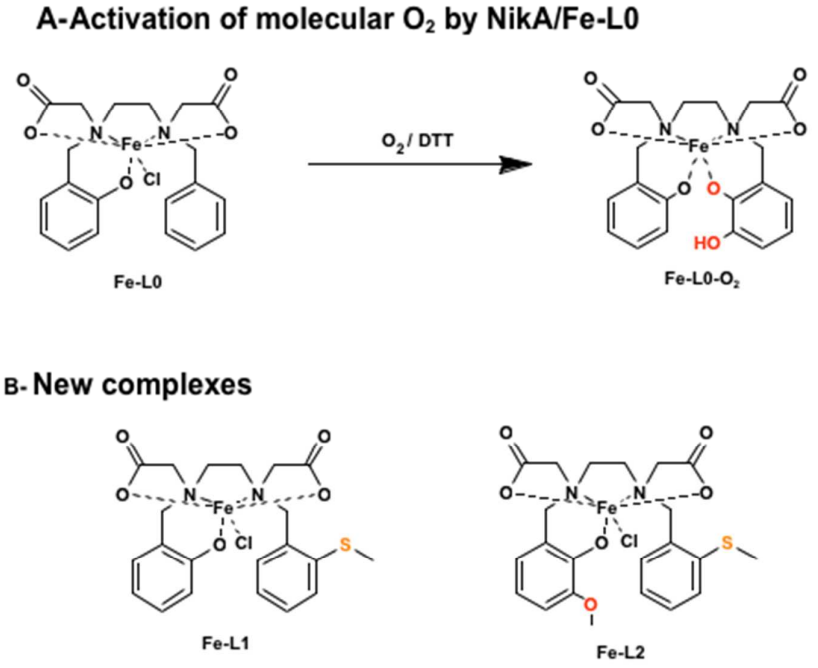

Results

Design of ligands L1 and L2

In this study, we took advantage of the reactivity of the iron complex **Fe-L0** (**L0** = *N*-benzyl-*N*'-(2-hydroxybenzyl)-*N*,*N*'-ethylene diamine diacetic acid), bound to NikA, that could perform a double intramolecular hydroxylation using dioxygen as the oxidant (Figure

1A). Our previous results showed that the binding of the reaction product – hydroxylated ligand - to the metal inhibited further binding of dioxygen and prevented the catalytic oxidation of exogenous substrates.[14] To circumvent this event, new ligands were designed to block these reactive positions in **L0**. Thus, the benzyl ring was replaced by a thiomethyl (SMe) moiety, whereas a methoxy substituent was added to the leaving *ortho* position of the phenol ring, generating the two ligands **L1** and **L2**, respectively (Figure 1B).

Structural characterization of NikA/Fe-L1 and NikA/Fe-L2 and reactivity toward O_2. X-ray structures of **NikA/Fe-L1**, **NikA/Fe-L2**, **NikA/Fe-L1-red**, **NikA/Fe-L2-red**, **NikA/Fe-L1-O_2** and **NikA/Fe-L2-O_2** were solved (Table S1A). The presence of **Fe-L1** and **Fe-L2** within the crystals was revealed by their red or purple color, respectively (Figure 2A). X-ray fluorescence experiments attested the presence of iron (Figure S3). The crystal structures of **NikA/Fe-L1** and **NikA/Fe-L2** showed that, in both cases, Fe(III) is hexacoordinated by three oxygen atoms from one phenolate and two carboxylates, the two nitrogen atoms from the ethylene-1,2-diamine moiety and a water molecule. Occupancies close to 1 could be assigned for Fe-**L1** and Fe-**L2** in both structures (Figure 2A). Binding of **Fe-L1** and **Fe-L2** to NikA involves a network of supramolecular interactions (Figure S1 and Table S1). The stronger interaction is mediated by a salt bridge formed between a carboxylate group of the ligand and Arginine 137. This carboxylate group is stabilized by an interaction with a structural water, bound to Tyrosine 402. In addition, π-stacking interactions are possible with Tryptophan 398, as previously observed with **Fe-L0**. Moreover, from a previous study,[12] potential weak CH/π interactions between **L1** or **L2** and Histidine 416, Tryptophan 100 and Tryptophan 398 would help the stabilization of **Fe-L1** and **Fe-L2** in NikA's binding pocket. To obtain the ferrous state compatible with dioxygen activation,[14] **NikA/Fe-Lx** crystals were soaked for 60 minutes in 50 mM DTT in a glove box under anaerobic conditions. After this step, the crystals were practically colorless (Figure 2B). The reduction step did not lead to the release of either the iron or the complexes, since the occupancy for **Fe-L1** and **Fe-L2** remained close to 1. In both structures, Fe(II) was found to be hexacoordinated with three oxygen atoms from one phenolate and two carboxylates, the two nitrogen atoms from the ethylene-1,2-diamine moiety and potentially, the sulfur atom of the SMe group (d Fe-S = 2.4-2.6 Å) (**NikA/Fe-Lx-Red**, Figure 2B). A similar methionine thioether coordination of iron, with a distance of 2.57 Å, was described in isopenicillin N synthase.[15] This octahedral coordination resulted from the Fe(III) to Fe(II) redox transition which induced a conformational change in the ligand. Thus, the substituted phenyl ring moved to the apical position, previously occupied by

a carboxylate group, which formed a new salt bridge with Arg97 to compensate for the loss of charge of the complex. The conformational change observed was different to that in the **NikA/Fe-L0-Red** structure, where the whole coordination sphere was affected, with the phenyl ring replacing the phenol ring.[14]

Figure 2. Crystal structures and dioxygen-reactivity of NikA/Fe-Lx hybrids.

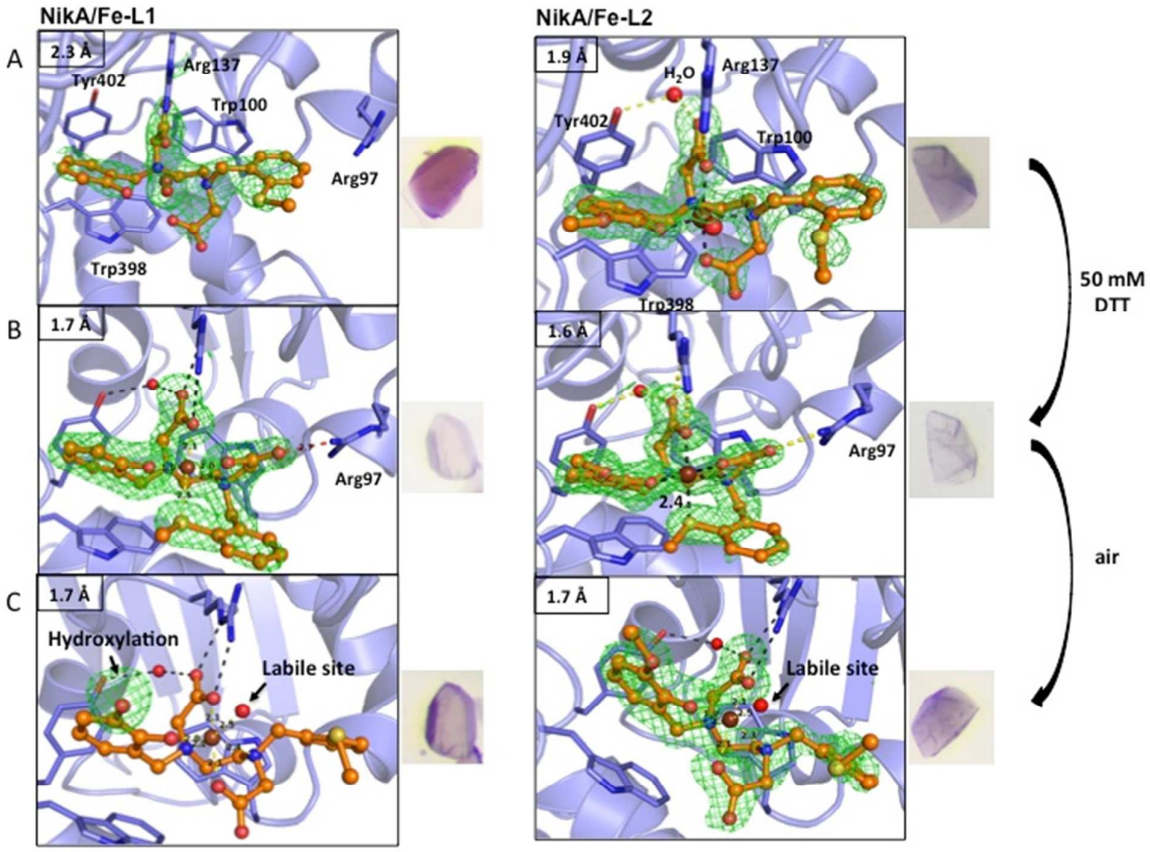

Crystal structures, OMIT Fourier electron density maps and crystal images of **NikA/Fe-Lx** hybrids at different reaction stages. (A) **NikA/Fe-Lx**. (B) **NikA/Fe-Lx-red**: Reduced **NikA/Fe-Lx** after soaking for 60 min in an artificial mother liquor containing 50 mM DTT. (C) **NikA/Fe-Lx-O_2**: **NikA/Fe-Lx-red** after exposure to air for 4 hours. Electron density maps (shown in green) are contoured to 3s. For clarity, in figure 2C, OMIT Fourier electron density map was calculated with a model containing L1 to highlight the presence of the hydroxyl group. Ligands Lx are depicted in orange, and iron is illustrated by a brown sphere. Water molecules are depicted as red spheres. Amino-acids constituting the complex-binding site are shown as blue sticks. The interaction distances between Fe and ligands are indicated in Table S1B).

When **NikA/Fe-L1-red** or **NikA/Fe-L2-red** crystals were subsequently exposed to air, the color changed from colorless to purple in both cases (**NikA/Fe-Lx-O_2**, Figure 2C). A color transition from red to purple was also observed when **NikA/Fe-L1** crystals were soaked in a DTT solution under aerobic conditions, yielding **NikA/Fe-L1-O_2** crystals. Using the same method, no color change was observed when **NikA/Fe-L2** was transformed into **NikA-**

Fe-L2-O_2. In the case of **NikA/Fe-L1-O_2,** the crystal structure showed an additional electron density modelled as a single intramolecular hydroxylation of the phenol group at the *meta* position producing catechol as the sole product of the reaction.[§] In contrast, the **NikA/Fe-L2-O_2** structure showed no intramolecular hydroxylation (Figure 2C) and was therefore similar to the initial **NikA/Fe-L2** since, unlike **L1**, **L2** lacks a C-H group close enough to be directly attacked by the iron-based oxidative species. In both **NikA/Fe-L2-O_2** and **NikA/Fe-L1-O_2** structures, an exchangeable position, necessary to dioxygen activation, is present in the coordination sphere of the iron. This position was modeled as a water molecule. Therefore, unlike **NikA/Fe-L0**, the two new artificial enzymes **NikA/Fe-L1** and **NikA/Fe-L2** can potentially perform oxidation reactions on exogenous substrates.

Oxidation of carbon-carbon double bonds by NikA/Fe-L2 CLEC with O_2 as the oxidant.

To increase the stability of the hybrids in organic solvents, CLEC technology was applied, making it possible to use a large range of water-insoluble substrates for catalysis. After cross-linking, the CLEC were stable for several months in a mixture of water and organic solvents. The integrity of **NikA/Fe-Lx CLEC** was verified by X-ray crystallography and X-ray fluorescence (Figures S4 and S5, respectively) before they were used in catalysis. Occupancy of 1 could be assigned for **L0**, **L1**, **L2** and iron in the three protein structures. Furthermore, protein-bound iron content was determined under reducing conditions with bathophenantroline disulfonate after acidic treatment of **NikA/Fe-L2 CLEC**,[16] revealing a close to 1:1 ratio between iron and the concentration of protein measured by SEC-MALLS (see SI).

We assessed the ability of **NikA/Fe-L2 CLEC**, the most stable hybrid under dioxygen, to activate molecular dioxygen in the presence of DTT, and to oxidize the carbon-carbon double bond in β-methoxystyrene, an enol ether of 2-phenylacetaldehyde (Table 1). Two products were obtained, benzaldehyde and 2-methoxyacetophenone, at yields of 38 and 36%, respectively, for a total TON of 550 (entry 1). In the absence of CLEC, no products were detected (entry 4). Moreover, the use of Ni-EDTA, a previously described ligand for NikA,[17] instead of **Fe-L2** led to an inactive **NikA/Ni-EDTA CLEC** (entry 5). Consequently, the efficiency of CLEC catalyst depends upon the iron complex inserted and the glutaraldehyde treatment doesn't affect the reactivity. Remarkably, **NikA/Fe-L2 CLEC** was more efficient than either **Fe-L2** or **NikA/Fe-L2**, which only performed 130 TON (entries 2-3) over 90 minutes. We next expanded the range of substrate to alkenes, and exclusively oxidative cleavage was obtained with yields of between 0 and 26% (entries 6-10-14-18-21). It

is worth mentioning that with alkene substrates the reaction could only be catalyzed by the CLEC system. Under the same conditions, cyclic aromatic double bonds in indene and 1,2-dihydronaphthalene and aliphatic alkenes were not oxidized. Allowing a longer reaction time (24 h) only benefited α-methylstyrene and 4-methoxystyrene transformations (yield of 27% and 51%, respectively, table 1, entries 6 and 10). The electronic effect of various substituents on the phenyl ring of the styrenyl derivatives drove the reactivity of the double bond, in line with an electrophilic addition.

Table 1. Oxidation of styrene derivatives by O_2.

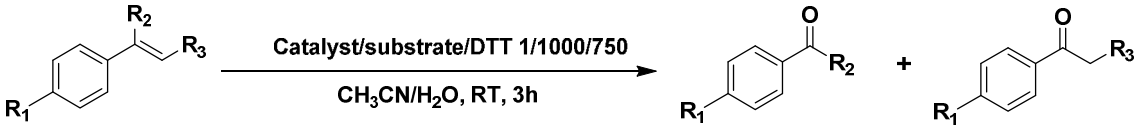

Entry	Substrate	Catalyst	Aldehyde[b] (%)	Ketone[b] (%)	TON[c]
1	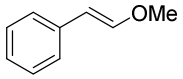	**NikA/Fe-L2 CLEC**	38	36	550
2		**Fe-L2**	8	9	130
3		**NikA/Fe-L2** hybrid[a]	11	6	130
4		-	0	0	0
5		**NikA/Ni-EDTA CLEC**	0	0	0
6	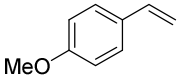	**NikA/Fe-L2 CLEC**	26(51[d])	0	200
7		**Fe-L2**	2	0	5
8		**NikA/Fe-L2** hybrid[a]	6	0	50
9		-	0	0	0
10	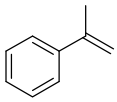	**NikA/Fe-L2 CLEC**	0	7(27[d])	50
11		**Fe-L2**	0	0	0
12		**NikA/Fe-L2** hybrid[a]	0	0	0
13		-	0	0	0
14	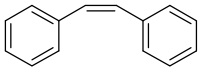	**NikA/Fe-L2 CLEC**	22	0	170
15		**Fe-L2**	0	0	0
16		**NikA/Fe-L2** hybrid[a]	0	0	0
17		-	0	0	0
18	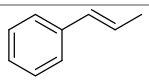	**NikA/Fe-L2 CLEC**	2	0	15
19		**Fe-L2**	0	0	0
20	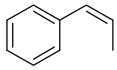	**NikA/Fe-L2 CLEC**	0	0	0
21		**Fe-L2**	0	0	0

[a] Catalysis was performed in HEPES buffer 10 mM pH 7.5. [b] Yield calculated relative to initial DTT concentration. [c] Errors evaluated to 14% (see experimental section). [d] Yield after 24 h.

Furthermore, the reaction was reductant-dependent. Thus, a direct correlation between product yield and DTT concentration was observed, with a correlation factor close to one (Figure S6) for *β*-methoxystyrene oxidation. Other reductants, such as ascorbate or TCEP, were ineffective under the experimental conditions tested. Reducing the metal prior to substrate exposure with only 10 equivalents of DTT, to allow direct O_2 activation, was also incompatible with catalysis (less than 2% yield).

Kinetics revealed a lag phase of about 30 minutes for **NikA/Fe-L2 CLEC** and **Fe-L2** (Figure S7A and B). Pre-incubation of both catalysts with DTT under anaerobic conditions before adding substrate eliminated this lag phase and the reaction was completed, indicating that reduction of the ferric state represents a rate limiting step for the reaction (Figure S8). ^{18}O-labeled water was used to discriminate between potential oxidative pathways. None of the products (aldehyde or ketone) produced from *β*-methoxystyrene or *cis*-stilbene were ^{18}O-labeled, indicating that the oxygen atoms inserted were derived from $^{16}O_2$ (see SI). Furthermore, addition of DMPO (75% *vs.* the substrate) completely inhibited the formation of any products, whatever the substrate, demonstrating that the reaction involves radicals. However, no DMPO-OH• or DMPO-OOH• radicals could be identified by EPR, suggesting that free oxygenated radicals are not produced during the process.

Stability experiments were performed with the different catalysts. The activity of the **NikA/Fe-L2** decreased drastically in buffered medium with 210 TON performed over 3 runs (Figure 3A). **Fe-L2** was slightly more efficient, with 540 TON performed over 6 runs. Remarkably, **NikA/Fe-L2 CLEC** remained fully active even after 50 successive runs, with more than 28 000 TON performed with no loss of activity (Figure 3A). X-ray fluorescence spectra showed the persistent presence of iron in **NikA/Fe-L2 CLEC** after 20 runs, confirming that the catalyst was mostly retained in the crystal (Figure S5). Moreover, the kinetics of the reaction were unaltered during successive runs, emphasizing the absence of leaching of the catalyst (Figure S7C). In contrast, a steady loss of catalytic efficiency was observed with **NikA/Fe-L0 CLEC** and **NikA/Fe-L1 CLEC** after 8 and 12 runs, respectively, indicating that the catalytic reaction is centered on the iron complex and that the efficiency (35% yield for **NikA/Fe-L0 CLEC** and 42% yield for **NikA/Fe-L1 CLEC**) and stability are complex-dependent (Figure 3B).

Figure 3. Stability experiments relating to O_2/DTT reactivity.

A. NikA/Fe-L2 CLEC *vs.* Fe-L2 and NikA/Fe-L2 hybrid.

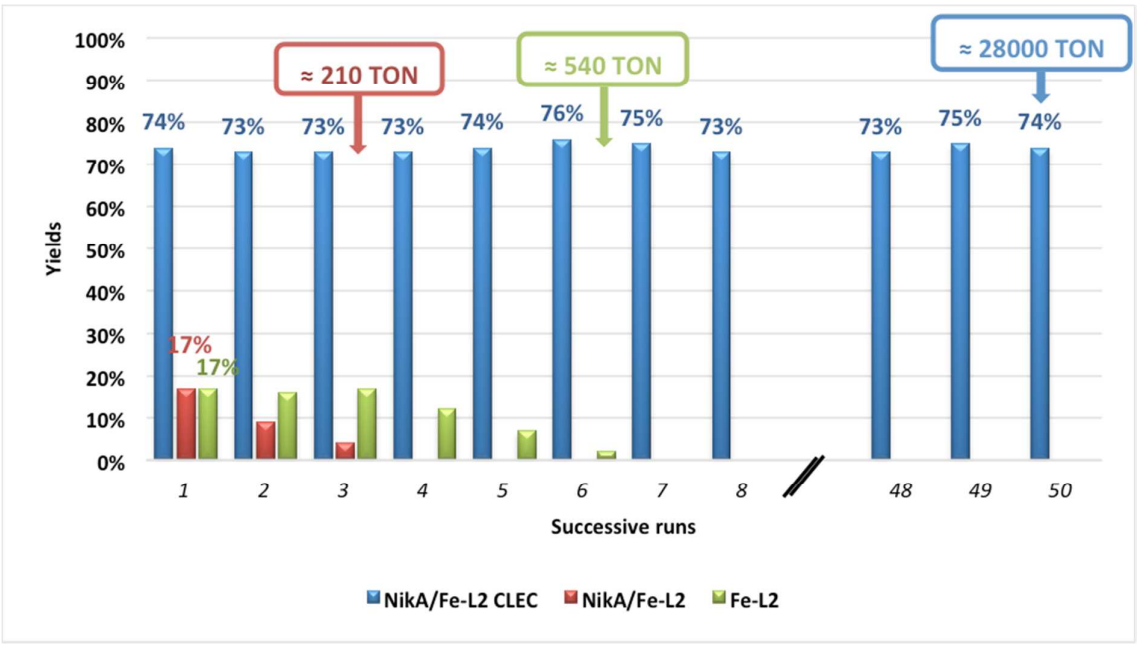

B. NikA/Fe-L2 *vs.* NikA/Fe-L1 and NikA/Fe-L0.

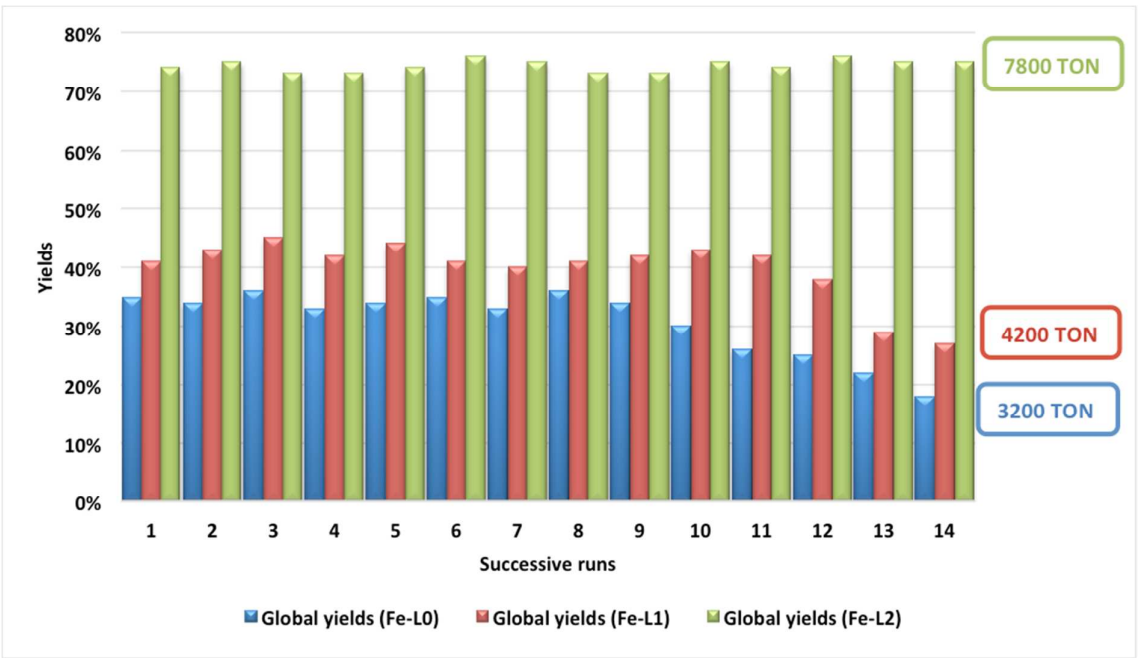

Reaction performed with β-methoxystyrene. Each point is a standard reaction, always using the same batch of 100 CLEC (see Experimental Section). Ratio Catalyst/Substrate/DTT: 1/1000/750, 3 h, [CLEC] = 31 μM in acetonitrile:water 1:1.

Optimization of the catalytic properties of NikA/Fe-L2 CLEC towards chlorohydrin production.

To evaluate the catalytic efficiency of CLEC for double bond transformations, we screened a range of oxidants to monitor the oxidation of enol ether and α-methylstyrene, +/- chloride for potential chlorohydrin formation (Table S2). H_2O_2, CH_3CO_3H and *t*-BuOOH were inefficient, whereas $KHSO_5$, NaOCl and *m*-CPBA provided reasonable conversion and selectivity. $KHSO_5$ and *m*-CPBA allowed production of equimolar amounts of ketone and aldehyde from *β*-methoxystyrene, with a slightly lower conversion than during reductive dioxygen activation. In the case of α-methylstyrene, low conversion (less than 15% yield) and/or moderate chemoselectivity (around 75%) were observed. Conversely, in the presence of chloride, $KHSO_5$ was identified as the most promising oxidant as it produced a chemo- and regio-selective hydroxychlorination yielding 1-chloro-2-phenylpropan-2-ol as sole product (Table 2, entry 1). As controls, **Fe-L2** alone and **NikA/Ni-EDTA CLEC** were found quasi inactive, demonstrating that the reaction was driven by **NikA/Fe-L2 CLEC**.

A series of styrene derivatives were effectively hydroxychlorinated with exclusive Markovnikov regioselectivity (Table 2). However, chemoselectivity varied between 29% and 100% as a dichlorinated product was also detected (for *cis*-stilbene and 4-methoxystyrene, respectively). Styrenyl substrates with an electron-donating moiety were attacked to give quasi-quantitative yields; for example 4-methoxystyrene was transformed into 2-chloro-1-(4-methoxyphenyl)-ethanol in 30 min (480 TON, entry 4). However, when substrates contained an electron-withdrawing substituent such as 4-bromostyrene, the reaction was drastically slowed, producing only 4% of chlorohydrin product after 30 min, and 26% in 14 hours (entry 5). These results indicate that the reaction is favored in the case of electron-rich double bonds, hinting at the electrophilic nature of the oxidative species. As a consequence, the reaction of aliphatic cyclic alkenes such as methylcyclohexene resulted in a low yield of chlorohydrin (only 5%, entry 9). *E-Z* stereoisomerism did not impact the yield of the reaction, but did affect chemoselectivity, since *trans*-ß-methylstyrene gave 92% while the *cis-β*-methylstyrene only produced 79% (entries 2 and 3). An effect of steric hindrance was also observed, with stilbenes only providing low yields (41% for the *cis*- and 19% for the *trans*- isomers, entries 7 and 8) and rather poor chemoselectivity. **NikA/Fe-L2 CLEC** led to very high diastereoselectivity (100:0 in favor of the *trans* diastereomeric pair), but poor enantioselectivity as hydroxychlorination of the most rigid substrate, 1,2-dihydronaphthalene (entry 6), produced only 10% *ee* (Figure S9).

Table 2. Range of substrates tested with NikA/Fe-L2 CLEC

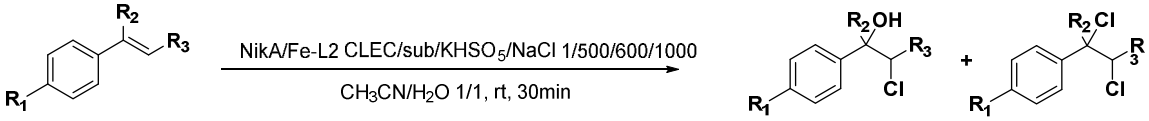

Entry	Substrate	Yield[a] (%)	TON[b]	Selectivity[c] (%)
1		98	490	80
2		75	380	79
3	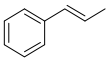	72	360	92
4	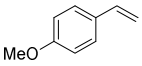	96	480	100
5	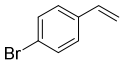	4(26[d])	20	100
6		97[e]	490	100
7	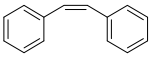	41	200	29
8	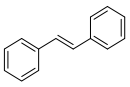	19	100	37
9		5[f]	30	100

Ratio Catalyst/Substrate/Oxidant/Chloride: 1/1000/750/1500, 30 min, [CLEC] = 31 μM in acetonitrile:water 1:1. [a] Yield calculated relative to initial $KHSO_5$ concentration. [b] Errors evaluated to 14% (see experimental section). [c] % of chlorohydrin relative to dichlorinated product. [d] Reaction time = 14 h. [e] *ee* = 10%. [f] When methylcyclohexene is used product is 2-chloro-1-methylcyclohexan-1-ol.

The conversion yield of 4-methoxystyrene was complex-dependent (Figure 4). The yield was significantly decreased with **NikA/Fe-L0 CLEC** (17% yield *i.e.*, 130 TON *vs.* 84% yield of chlorohydrin product *i.e.*, 630 TON with **NikA/Fe-L1 CLEC)**. Although the yield and TON were similar with **NikA/Fe-L2 CLEC**, the kinetics of 2-chloro-1-(4-methoxyphenyl)-ethanol production by **NikA/Fe-L1 CLEC** was slightly faster, with a TOF of 6500 h^{-1} (4600 h^{-1} for **NikA/Fe-L2 CLEC**) (Figure S10). Increasing the temperature from 20 to 70 °C resulted in a seven-fold increase in yield after only one minute of reaction (Figure S11A).

The stability of the three CLEC systems was tested during conversion of 4-methoxystyrene (Figure 4). With **NikA/Fe-L0 CLEC**, the reactivity rapidly decreased during

the three first catalytic runs (only 4% yield during the third run), with a total TON of 270. **NikA/Fe-L1 CLEC** retained full activity over 3 catalytic runs but then decreased drastically; a total of 3200 TON were performed over 13 catalytic runs. In comparison, **NikA/ Fe-L2 CLEC** retained full activity over 7 catalytic runs (and 3 runs at 70 °C, Figure S11B) and then decreased progressively, performing 5900 TON over 13 catalytic runs. Activity decreased as the crystals were bleached from purple to light yellow, corresponding to the loss of iron, as shown by X-ray fluorescence (Figure S5). In a second experiment, **NikA/Fe-L2 CLEC** were soaked in **Fe-L2** at runs 7, 9, 11 and 13. In these conditions, the catalytic efficiency remained stable for 9 runs, with yields decreasing slightly from 84% to 70% in the tenth run for a total of 6600 TON over 13 runs (Figure S12). Beyond 13 catalytic runs, **NikA/Fe-L2 CLEC** were practically inactive despite additional **Fe-L2** soaking. This result suggests that the full system underwent some oxidative damage. Soaking **NikA/Fe-L2 CLEC** in $FeCl_3$ at runs 7, 9, 11 and 13 had no effect on activity (Figure S13), indicating that the decrease in activity following several runs was related to loss or degradation of the full complex.

Figure 4. Stability experiments for hydroxychlorination of 4-methoxystyrene by NikA/Fe-Lx CLEC.

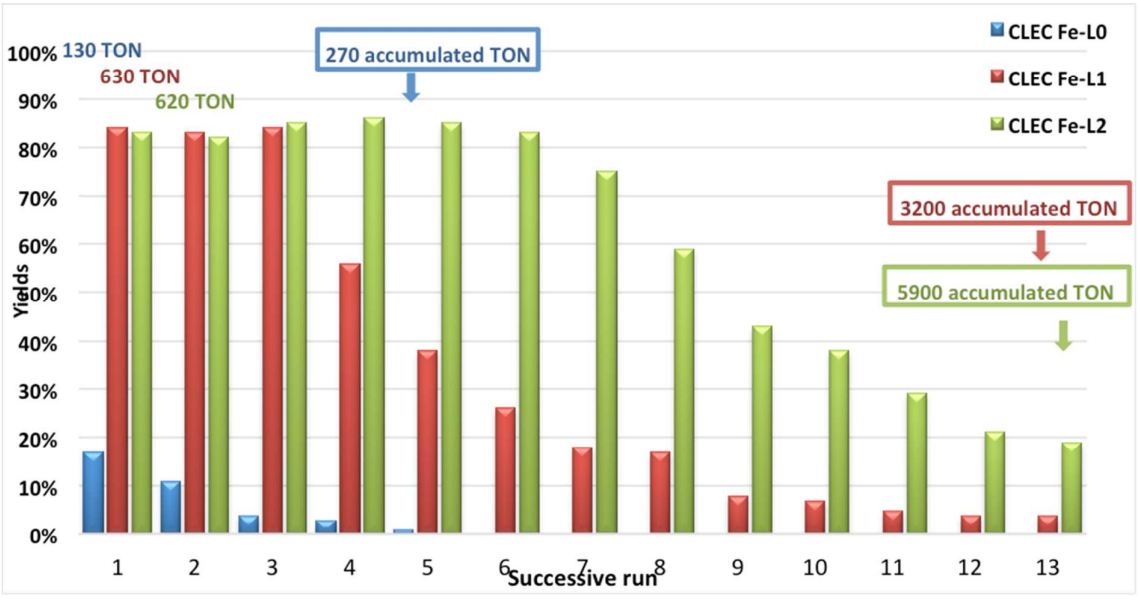

Reaction performed on 4-methoxystyrene. Each point is a standard reaction always using the same batch of 100 CLEC (see Experimental Section). Ratio Catalyst/Substrate/Oxidant/Chloride: 1/1000/750/1500, 30 min, [CLEC] = 31 µM in acetonitrile:water 1:1.

Raising the pH from 2.5 (pH value in the standard catalytic conditions) to 6.0 inhibited the hydroxychlorination reaction, thus only alcohols and carboxylic acids could be used as nucleophiles (Figure S14). Labeling experiments using $H_2{}^{18}O$ confirmed the existence of a

nucleophilic attack (the final product contained 85% oxygen-labeled 2-chloro-1-(4-methoxyphenyl)-ethanol (Figure S15). Thus, the primary step in the reaction involves an electrophilic addition of a chloronium into the double bond produced by the metal-based activation by $KHSO_5$. This addition is compatible with the absence of inhibition by the radical scavenger DMPO, which excludes the formation of Cl•, SO_4• and OH• as reactive intermediates.[18] Monitoring the reaction of a mixture of $KHSO_5$ and NaCl by UV-visible *in the absence of substrate* (Figure S16) revealed a slow buildup of a unique transition at 310 nm, suggesting the presence of Cl_2;[19] free HOCl (λ_{max} = 240 nm)[20] or OCl^-(λ_{max} = 296 nm)[19] were undetectable. Cl_2 forms from the conversion of HOCl in acidic medium, and its appearance (as indicated by the 310 nm transition) was inhibited by the presence **NikA/Fe-L2 CLEC**.

Discussion

The CLEC reported here presents considerable assets for heterogeneous catalysis. The unexpected efficiency under oxidative conditions, even using $KHSO_5$ or NaOCl, are unprecedented in (bio)catalysis, except with some heme catalysts or isolated hemoenzymes.[21] Moreover, selective oxidation processes relying on O_2 are problematic since they involve radical chemistry, and synthetic metallic catalysts are inherently susceptible to degradation by oxygen-based radicals. However, with TOF values ranging from 2 to 30 min^{-1}, our hybrid systems are comparable with natural enzymes.[22] This efficiency can be explained by two main factors: first, the cross-linking method produces a robust NikA-based hybrid crystal that is highly stable even under strong acidic conditions and high temperatures. Second, the mesoporous character of the high-catalyst-content crystals considerably benefits the reactivity (Figure S2). Indeed, the easy diffusion of molecules within a crystal in buffered solution or organic solvents has been demonstrated. Moreover, glutaraldehyde treatment did not appear to dramatically alter the crystal packing or the network of solvent channels. Thus, the diffusion of substrates (DTT, oxidants, and **Fe-Lx**) in soaking experiments could be demonstrated by the high catalytic efficiencies of **NikA/Fe-Lx CLEC**. In addition, the solid phase should influence the kinetics of the catalysis, and consequently the efficiency, for several reasons: i) the active species is locally highly concentrated while dispersed in the solution either for the complex alone or the hybrid; ii) the use of enzymes is often limited by their poor stability under reaction conditions, especially in the field of oxidation. In this study, we showed that **NikA/Fe-Lx** hybrids in solution were poorly active because of the

requirement of organic solvent for the reaction. In the same way, the use of $KHSO_5$ under acidic conditions led to the immediate degradation of the hybrids; iii) in some cases, the complex may be activated by the protein scaffold.[14,23] The case of O_2/DTT is symptomatic of another aspect of the influence of the solid state, *i.e.*, the compartmentalization of the catalyst with respect to its substrates and reactants. For example, in solution, *cis*-stilbene and α-methylstyrene were not transformed by O_2 and only minor activity was observed with 4-methoxystyrene or *β*-methoxystyrene (yield 0 *vs.* 11%, 0 *vs.* 7%, 17 *vs.* 26% and 17 *vs.* 78%, respectively). The yield for competitive oxidation of DTT was clearly enhanced for homogeneous catalysts compared to CLEC catalysts when performing oxidative cleavage of alkenes (Figure S17). The better synchronization between O_2 reduction steps and alkene oxidation suggests controlled traffic of both substrate and DTT inside the crystal. The CLEC system also provided better chemo- and stereo-selectivity compared to in-solution **Fe-Lx** complexes, mainly by restricting intermolecular side reactions and the influence of the protein scaffold.

For cleavage of non-aromatic double bonds, O_2 is rarely used, particularly with iron-based catalysts.[24] In nature, all but one[25] of the non-heme or heme enzymes display a dioxygenase-type behavior.[26] In contrast, the oxidative catalytic cleavage induced by **NikA/Fe-Lx CLEC** resembles a monooxygenase behavior since it is reductant-dependent and a $2e^-$ oxidant can replace dioxygen (Table S2B). However, its expected products, epoxides or diols,[25] were not detected. Moreover, pure samples of diols or epoxides remained inert under our oxidative conditions. Altogether, these results suggest a novel mechanistic pathway. O_2 activation by the reduced form of **NikA/Fe-Lx CLEC** initially led to the formation of a transient iron superoxo species, prior to forming the peroxo adduct structurally characterized in our previous study.[14] Only the involvement of a peroxo adduct is compatible with both the radical nature and chemoselectivity of the reaction if an 'in cage' hydroxyl radical resulting from a homolytic cleavage of the O-O bond (no aromatic oxidation was detected and the substrate promiscuity is too low for free OH•).[27] Moreover, peroxo iron species should not develop radical chemistry.[28] High valent species such as Fe(IV)=O can be eliminated based on the absence of labeling scrambling.[29] Conversely, superoxo adducts have been identified as intermediates in radical-mediated oxidative alkene cleavage and were shown to be capable of electrophilic addition to double bonds.[24a,28a] In our case, the superoxo iron species or the "in cage" hydroxyl radical should be added to a carbon on the double bond to produce a benzyl radical at the *β* position that further reacts with dioxygen prior to cleavage. Identification of

the radical species and the reaction steps following radical formation on the substrate will need to be clarified, as will the mechanism for ketone formation from the enol.

Catalytic hydroxychlorination activity has rarely been observed with natural enzymes (mainly as a by-product of chloroperoxidases).[30] Here again, the **NikA/Fe-L2 CLEC** displayed a unique reactivity. Three mechanistic activation scenarii are possible (Scheme 1): i) activation of $KHSO_5$ by **Fe-L2** following its binding and hetero- or homo-lytic cleavage of the O-O(S)O_2 bond. Homolytic cleavage should lead to radical chemistry and is therefore excluded in this case. (ii) **FeL2** plays the role of a Lewis acid activating the proximal oxygen (then being more positive) of an interacting SO_5^{-}. A direct attack of the chloride anion would generate the (H)OCl species either free in acidic medium or coordinated with the iron. The absence of reactivity when OCl^- was substituted for $KHSO_5$ precludes the existence of this iron species. HOCl has generally been proposed to be the oxidizing species with $KHSO_5$, but in our case the chemoselectivity observed was different (4-bromostyrene and cyclic alkenes were inert in this study).[31] iii) Metal-based polarization of Cl_2 produced from HOCl, which is the pathway we favor.

Scheme 1. Possible pathways of $KHSO_5$ activation to generate Cl_2 as the chloronium source.

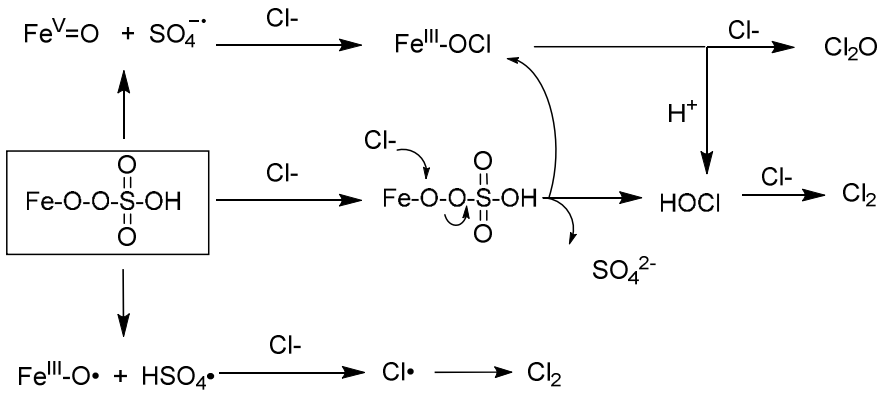

Conclusions

In this article we describe and characterize the first CLEC with artificial enzymes capable of performing an oxidation reaction. The stability of the biomaterial enables very complex reactions, such as selective catalysis by O_2 activation. The final asset of our approach lies in the straightforward the preparation of our hybrid based on supramolecular interactions, allowing easy loading or exchange of the inorganic catalyst. With this technology, new ways to use modular NikA-based CLEC are opened, with a broad scope of

complexes to perform a wide range of reactions in organic solvents. More importantly, the increased stability compared to enzymes in solution (pH, temperature, oxidation conditions) should extend the field for catalysis as an alternative to biocatalysis.

Experimental Section

Synthesis of ligands, complexes and products are described in SI.

Purification of NikA, crystallization and synthesis of cross-linked NikA/Fe-Lx crystals (NikA/Fe-Lx CLEC)

Cytoplasmic apo-NikA was purified as previously described.[32] **NikA/Fe-L1**, **NikA/Fe-L2**, **NikA/Fe-L0** and **NikA/Ni-EDTA** crystals were obtained as previously described for **NikA/Fe-L0**.[14]

NikA/Fe-Lx and **NikA/Ni-EDTA** crystals were cross-linked in 5% glutaraldehyde, 2.1 M ammonium sulfate and 100 mM Tris-HCl pH 7.0 for 5 h. Typically, crystals were soaked by addition of 5 µL of a solution of 10% glutaraldehyde in 2.1 M ammonium sulfate and 100 mM Tris-HCl pH 7.0. Then, **NikA/Fe-Lx CLEC** were transferred to a 50%, (v/v) CH_3CN/H_2O solution for catalysis experiments. For crystallographic studies, **NikA/Fe-Lx CLEC** were transferred to a 30% (v/v) glycerol/H_2O solution before flash cooling in liquid nitrogen.

Crystallographic studies of NikA/Fe-Lx in the presence of DTT and O_2

NikA/Fe-L1 and **NikA/Fe-L2** crystals were transferred to an anaerobic glove box (Jacomex) and soaked in an artificial mother liquor containing 100 mM Tris-HCl pH 7.0, 2.1 M ammonium sulfate, mixed with 50 mM DTT. After soaking for 60 min, the colorless reduced **NikA/Fe-Lx-red** crystals were exposed to air for four hours to yield **NikA/Fe-Lx-O_2** crystals. **NikA/Fe-Lx** crystals were also soaked four hours in the mother liquor containing 50 mM DTT in the presence of air to yield **NikA/Fe-Lx-O_2** crystals. All crystals were cryo-protected by adding 25% (v/v) glycerol to the mother liquor before flash cooling in liquid nitrogen.

Representative procedure for O_2 activation for a 1/1000/750 (catalyst/substrate/DTT) ratio with CLEC.

100 **NikA/Fe-Lx CLEC**, fished directly from the soaking solution, were washed twice in 1 mL of acetonitrile/water 1:1 solution. The supernatant was removed, leaving a final volume of 37 µL. Then, 1.5 µL of a 0.82 M solution of substrate (1.23 µmol) in 100% acetonitrile and

1.5 µL of a 0.62 M DTT solution (0.92 µmol) were added successively, resulting in a final volume of 40 µL. The reaction was stirred at room temperature for 3 hours, 1.5 µL of benzophenone 0.1 M was added and the reaction mixture was extracted with AcOEt (60 µL). The organic phase was analyzed by GC/MS. The final concentration of CLEC was 31 ± 5 µM based on MALLS measurements.

Representative procedure for hydroxychlorination catalysis for a 1/500/600/1000 Catalyst/Substrate/Oxidant/Chloride (C/S/O/Cl) ratio with CLEC

100 **NikA-Fe-Lx CLEC** were washed twice in 1 mL of acetonitrile/water 1:1 solution. The supernatant was removed, leaving a final volume of 30 µL. Then 1.5 µL of a 0.41 M solution of substrate (0.615 µmol) in 100% acetonitrile, 4 µL of a 0.31 M sodium chloride solution (1.23 µmol) and 5 µL of a 0.29 M $KHSO_5$ solution (0.725 µmol) were added successively to give a final volume of 40.5 µL. The final CLEC concentration was 31 ± 5 µM. The reaction was stirred at room temperature for 30 min, then 1.5 µL of benzophenone 0.1 M was added and the reaction mixture was extracted with AcOEt (60 µL). The organic phase was analyzed by GC/MS. A catalyst concentration of 31 µM was used to calculate ratios and determine TON and TOF. To monitor the kinetics, a reaction mixture was prepared for each point and was measured in duplicate. Reaction mixtures were prepared according to the above procedure. The TOF was calculated from the linear slope of the curve of the TON as a function of time between 0 and 3 minutes.

Stability experiments

For stability experiments, the standard procedures were applied for the first run. Then CLEC were washed with 1 mL of acetonitrile:water 1:1 and reused for the second run. The same procedure was applied for as many runs as possible. In the case of homogeneous catalysis, the oxidant and substrate were added on three separate samples: first, with an extraction after 90 min; second with an extraction after two successive additions; third with an extraction after three successive additions and so on. The mixture was then extracted with AcOEt and analyzed for its content.

For the reloading experiments, after runs 7, 9, 11 and 13, **NikA/Fe-L2 CLEC** were soaked in 50 µL of 5 mM $FeCl_3$ or **Fe-L2** solution for 3 h before washing three times with 1 mL of an acetonitrile/water 1:1 solution to remove excess free complex from the solution.

ACKNOWLEDGEMENTS

We thank the staffs from the BM-30A and ID30A-3 beamlines of the European Synchrotron Facility in Grenoble.

ASSOCIATED CONTENT

Supporting Information. Ligands and complexes synthesis and their physical characterization, crystal structures, catalytic procedures and kinetic data are reported. This material is available free of charge via the Internet at http://pubs.acs.org."

AUTHOR INFORMATION

Corresponding Author

* To whom correspondence should be addressed: christine.cavazza@cea.fr, stephane.menage@cea.fr

Funding Sources

This work was supported by the French National Agency for Research (grant ANR-14-CE06-0005-01), Labex ARCANE (ANR-11-LABEX-0003-1), and recurrent funding from CEA, CNRS and Univ. Grenoble-Alpes.

References

(1) a) Anastas, P. T.; Kirchhoff, M. M. *Acc. Chem. Res.* **2002**, *35*, 686; b) Poliakoff, M.; Fitzpatrick, J. M.; Farren, T. R.; Anastas, P. T. *Science* **2002**, *297*, 807; c) Sheldon, R. A. *Chem. Soc. Rev.* **2012**, *41*, 1437.

(2) a) Bornscheuer, U. T.; Huisman, G. W.; Kazlauskas, R. J.; Lutz, S.; Moore, J. C.; Robins, K. *Nature* **2012**, *485*, 185; b) Faber, K.; Kroutil, W. *Curr. Opin. Chem. Biol.* **2005**, *9*, 181; c) Nestl, B. M.; Hammer, S. C.; Nebel, B. A.; Hauer, B. *Angew. Chem. Int. Ed.* **2014**, *53*, 3070; d) Breuer, M.; Ditrich, K.; Habicher, T.; Hauer, B.; Keßeler, M.; Stürmer, R.; Zelinski, T. *Angew. Chem. Int. Ed.* **2004**, *43*, 788.

(3) a) Tran, D. N.; Balkus, K. J. *ACS Catal.* **2011**, *1*, 956; b) Sheldon, R. A.; van Pelt, S. *Chem. Soc. Rev.* **2013**, *42*, 6223; c) Garcia-Galan, C.; Berenguer-Murcia, Á.; Fernandez-Lafuente, R.; Rodrigues, R. C. *Adv. Synth. Cat.* **2011**, *353*, 2885.

(4) a) Yan, E.-K.; Cao, H.-L.; Zhang, C.-Y.; Lu, Q.-Q.; Ye, Y.-J.; He, J.; Huang, L.-J.; Yin, D.-C. *RSC Adv.* **2015**, *5*, 26163; b) Bornscheuer, U. T. *Angew. Chem. Int. Ed.* **2003**, *42*, 3336.

(5) Hanefeld, U.; Cao, L.; Magner, E. *Chem. Soc. Rev.* **2013**, *42*, 6211.

(6) a) Margolin, A. L.; Navia, M. A. *Angew. Chem. Int. Ed.* **2001**, *40*, 2204; b) Roy, J. J.; Abraham, E. T. *Chem. Rev.* **2004**, *104*, 3705; c) Quiocho, F. A.; Richards, F. M. *PNAS* **1964**, *52*, 833.

(7) Persichetti, R. A.; Clair, N. L. S.; Griffith, J. P.; Navia, M. A.; Margolin, A. L. *J. Am. Chem. Soc.* **1995**, *117*, 2732.

(8) a) Luiz de Mattos, I.; Lukachova, L. V.; Gorton, L.; Laurell, T.; Karyakin, A. A. *Talanta* **2001**, *54*, 963; b) Khalaf, N.; Govardhan, C. P.; Lalonde, J. J.; Persichetti, R. A.; Wang, Y.-F.; Margolin, A. L. *J. Am. Chem. Soc.* **1996**, *118*, 5494.

(9) Ayala, M.; Horjales, E.; Pickard, M. A.; Vazquez-Duhalt, R. *Biochem. Biophys. Res. Commun.* **2002**, *295*, 828.

(10) a) Yu, F.; Cangelosi, V. M.; Zastrow, M. L.; Tegoni, M.; Plegaria, J. S.; Tebo, A. G.; Mocny, C. S.; Ruckthong, L.; Qayyum, H.; Pecoraro, V. L. *Chem. Rev.* **2014**, *114*, 3495; b) Marchi-Delapierre, C.; Rondot, L.; Cavazza, C.; Ménage, S. *Isr. J. Chem.* **2015**, *55*, 61; c) Schwizer, F.; Okamoto, Y.; Heinisch, T.; Gu, Y.; Pellizzoni, M. M.; Lebrun, V.; Reuter, R.; Köhler, V.; Lewis, J. C.; Ward, T. R. *Chem. Rev.* **2017**, 10.1021/acs.chemrev.7b00014.

(11) a) Abe, S.; Maity, B.; Ueno, T. *Chem. Commun.* **2016**, *52*, 6496; b) Tabe, H.; Abe, S.; Hikage, T.; Kitagawa, S.; Ueno, T. *Chem. Asian J.* **2014**, *9*, 1373.

(12) Cherrier, M. V.; Girgenti, E.; Amara, P.; Iannello, M.; Marchi-Delapierre, C.; Fontecilla-Camps, J. C.; Menage, S.; Cavazza, C. *J. Biol. Inorg. Chem.* **2012**, *17*, 817.

(13) Bäckvall, J. E. *Modern Oxidation Methods*; Wiley-VCH, Weinheim, **2004**.
(14) Cavazza, C.; Bochot, C.; Rousselot-Pailley, P.; Carpentier, P.; Cherrier, M. V.; Martin, L.; Marchi-Delapierre, C.; Fontecilla-Camps, J. C.; Menage, S. *Nat. Chem.* **2010**, *2*, 1069.
(15) Clifton, I. J.; Ge, W.; Adlington, R. M.; Baldwin, J. E.; Rutledge, P. J. *Chembiochem* **2011**, *12*, 1881.
(16) Fish, W. W. *Methods Enzymol.* **1988**, *158*, 357.
(17) Addy, C.; Ohara, M.; Kawai, F.; Kidera, A.; Ikeguchi, M.; Fuchigami, S.; Osawa, M.; Shimada, I.; Park, S.-Y.; Tame, J. R. H.; Heddle, J. G. *Acta Crystallogr., Sect. D* **2007**, *63*, 221.
(18) Hussain, H.; Green, I. R.; Ahmed, I. *Chem. Rev.* **2013**, *113*, 3329.
(19) Wang, T. X.; Kelley, M. D.; Cooper, J. N.; Beckwith, R. C.; Margerum, D. W. *Inorg. Chem.* **1994**, *33*, 5872.
(20) Barnes, R. J.; Sinha, A.; Michelsen, H. A. *J. Phys. Chem. A* **1998**, *102*, 8855.
(21) a) Meunier, B.; de Visser, S. P.; Shaik, S. *Chem. Rev.* **2004**, *104*, 3947; b) *Handbook of porphyrin science*; Kadish, K.; Smith, K.; Guilard, R., Eds.; World Scientific, **2010**; Vol. 10; c) Urlacher, V. B.; Girhard, M. *Trends Biotechnol.* **2011**, *30*, 26; d) Fasan, R. *ACS Catal.* **2012**, *2*, 647.
(22) a) McAndrew, R. P.; Sathitsuksanoh, N.; Mbughuni, M. M.; Heins, R. A.; Pereira, J. H.; George, A.; Sale, K. L.; Fox, B. G.; Simmons, B. A.; Adams, P. D. *PNAS* **2016**, *113*, 14324; b) Chauhan, N.; Thackray, S. J.; Rafice, S. A.; Eaton, G.; Lee, M.; Efimov, I.; Basran, J.; Jenkins, P. R.; Mowat, C. G.; Chapman, S. K.; Raven, E. L. *J. Am. Chem. Soc.* **2009**, *131*, 4186.
(23) a) Rousselot-Pailley, P.; Bochot, C.; Marchi-Delapierre, C.; Jorge-Robin, A.; Martin, L.; Fontecilla-Camps, J. C.; Cavazza, C.; Menage, S. *Chembiochem* **2009**, *10*, 545; b) Esmieu, C.; Cherrier, M. V.; Amara, P.; Girgenti, E.; Marchi-Delapierre, C.; Oddon, F.; Iannello, M.; Jorge-Robin, A.; Cavazza, C.; Ménage, S. *Angew. Chem. Int. Ed.* **2013**, *52*, 3922; c) Rondot, L.; Girgenti, E.; Oddon, F.; Marchi-Delapierre, C.; Jorge-Robin, A.; Ménage, S. *J. Mol. Catal. A: Chem.* **2016**, *416*, 20; d) Lopez, S.; Rondot, L.; Cavazza, C.; Iannello, M.; Boeri-Erba, E.; Burzlaff, N.; Strinitz, F.; Jorge-Robin, A.; Marchi-Delapierre, C.; Menage, S. *Chem. Commun.* **2017**, *53*, 3579.
(24) a) Spannring, P.; Bruijnincx, P. C. A.; Weckhuysen, B. M.; Klein Gebbink, R. J. M. *Catal. Sci. Technol.* **2014**, *4*, 2182; b) Chen, H.; Ji, H.; Zhou, X.; Xu, J.; Wang, L. *Catal. Commun.* **2009**, *10*, 828.
(25) Marasco, E. K.; Schmidt-Dannert, C. *Chembiochem* **2008**, *9*, 1450.
(26) a) Rajagopalan, A.; Lara, M.; Kroutil, W. *Adv. Synth. Cat.* **2013**, *355*, 3321; b) Geng, J.; Liu, A. *Arch. Biochem. Biophys.* **2014**, *544*, 18; c) Harrison, P. J.; Bugg, T. D. H. *Arch. Biochem. Biophys.* **2014**, *544*, 105.
(27) a) Bach, R. D.; Dmitrenko, O. *J. Am. Chem. Soc.* **2006**, *128*, 1474; b) Bach, R. D.; Dmitrenko, O. *J. Org. Chem.* **2010**, *75*, 3705.
(28) a) Ray, K.; Pfaff, F. F.; Wang, B.; Nam, W. *J. Am. Chem. Soc.* **2014**, *136*, 13942; b) Oloo, W. N.; Que, L. *Acc. Chem. Res.* **2015**, *48*, 2612.
(29) a) Seo, M. S.; In, J. H.; Kim, S. O.; Oh, N. Y.; Hong, J.; Kim, J.; Que, L.; Nam, W. *Angew. Chem. Int. Ed.* **2004**, *43*, 2417; b) Jensen, M. P.; Lange, S. J.; Mehn, M. P.; Que, E. L.; Que, L. *J. Am. Chem. Soc.* **2003**, *125*, 2113.
(30) a) Vaillancourt, F. H.; Yeh, E.; Vosburg, D. A.; Garneau-Tsodikova, S.; Walsh, C. T. *Chem. Rev.* **2006**, *106*, 3364; b) Butler, A.; Sandy, M. *Nature* **2009**, *460*, 848.
(31) Swamy, P.; Kumar, M. A.; Reddy, M. M.; Naresh, M.; Srujana, K.; Narender, N. *RSC Advances* **2014**, *4*, 26288.
(32) Cherrier, M. V.; Cavazza, C.; Bochot, C.; Lemaire, D.; Fontecilla-Camps, J. C. *Biochemistry* **2008**, *47*, 9937.

[§§] The oxygen insertion was proposed on the basis of a previous study (reference 14) and on mass spectrometry study of O_2 activation of **Fe-L1** alone in aqueous solution (Figure S18).

Graphic for TOC.